Pseudorapidity Distributions of Charged Particles from Au + Au Collisions at the Maximum RHIC Energy, $\sqrt{s_{NN}} = 200$ GeV

I. G. Bearden,[7] D. Beavis,[1] C. Besliu,[10] Y. Blyakhman,[6] B. Budick,[6] H. Bøggild,[7] C. Chasman,[1] C. H. Christensen,[7] P. Christiansen,[7] J. Cibor,[3] R. Debbe,[1] E. Enger,[12] J. J. Gaardhøje,[7] K. Hagel,[8] O. Hansen,[7] A. Holm,[7] A. K. Holme,[12] H. Ito,[11] E. Jakobsen,[7] A. Jipa,[10] J. I. Jørdre,[9] F. Jundt,[2] C. E. Jørgensen,[7] R. Karabowicz,[4] T. Keutgen,[8] E. J. Kim,[1] T. Kozik,[4] T. M. Larsen,[12] J. H. Lee,[1] Y. K. Lee,[5] G. Løvhøiden,[12] Z. Majka,[4] A. Makeev,[8] B. McBreen,[1] M. Mikelsen,[12] M. Murray,[8] J. Natowitz,[8] B. S. Nielsen,[7] J. Norris,[11] K. Olchanski,[1] J. Olness,[1] D. Ouerdane,[7] R. Płaneta,[4] F. Rami,[2] C. Ristea,[10] D. Röhrich,[9] B. H. Samset,[12] D. Sandberg,[7] S. J. Sanders,[11] R. A. Sheetz,[1] P. Staszel,[7] T. F. Thorsteinsen,[9,*] T. S. Tveter,[12] F. Videbæk,[1] R. Wada,[8] A. Wieloch,[4] and I. S. Zgura[10]
(BRAHMS Collaboration)

[1]*Brookhaven National Laboratory, Upton, New York 11973*
[2]*Institut de Recherches Subatomiques and Université Louis Pasteur, Strasbourg, France*
[3]*Institute of Nuclear Physics, Krakow, Poland*
[4]*Jagiellonian University, Krakow, Poland*
[5]*Johns Hopkins University, Baltimore, Maryland 21218*
[6]*New York University, New York, New York 10003*
[7]*Niels Bohr Institute, University of Copenhagen, Copenhagen, Denmark*
[8]*Texas A&M University, College Station, Texas 77843*
[9]*University of Bergen, Department of Physics, Bergen, Norway*
[10]*University of Bucharest, Bucharest, Romania*
[11]*University of Kansas, Lawrence, Kansas 66045*
[12]*University of Oslo, Department of Physics, Oslo, Norway*

(Received 3 December 2001; revised manuscript received 14 February 2002; published 2 May 2002)

We present charged-particle multiplicities as a function of pseudorapidity and collision centrality for the ^{197}Au + ^{197}Au reaction at $\sqrt{s_{NN}} = 200$ GeV. For the 5% most central events we obtain $dN_{\rm ch}/d\eta|_{\eta=0} = 625 \pm 55$ and $N_{\rm ch}|_{-4.7\le\eta\le4.7} = 4630 \pm 370$, i.e., 14% and 21% increases, respectively, relative to $\sqrt{s_{NN}} = 130$ GeV collisions. Charged-particle production per pair of participant nucleons is found to increase from peripheral to central collisions around midrapidity. These results constrain current models of particle production at the highest RHIC energy.

DOI: 10.1103/PhysRevLett.88.202301 PACS numbers: 25.75.Dw

A central question in the study of collisions between heavy nuclei at the maximum energy of the Relativistic Heavy Ion Collider (RHIC) facility, $\sqrt{s_{NN}} = 200$ GeV, is the role of hard scatterings between partons and the interactions of these partons in a high-density environment. A reduction in the number of hadrons at large transverse momentum has already been observed for $\sqrt{s_{NN}} = 130$ GeV collisions that may hint at suppression of hadronic jets at high matter densities [1,2]. More generally, it has been conjectured that new phenomena related to nonperturbative QCD may occur at the highest RHIC energy. For example, a saturation of the number of parton collisions in central nucleus-nucleus collisions could lead to a limit on the production of charged particles [3–5].

This Letter addresses these issues with the first comprehensive investigation of multiplicity distributions of emitted charged particles in relativistic collisions between ^{197}Au nuclei with $\sqrt{s_{NN}} = 200$ GeV. In particular, we have measured pseudorapidity distributions of charged particles $dN_{\rm ch}/d\eta$ in the range $-4.7 \le \eta \le 4.7$ as a function of collision centrality. The pseudorapidity variable η is related to the particle emission angle θ with $\eta = -\ln[\tan(\theta/2)]$. We find that the production of charged particles at midrapidity ($\eta \approx 0$) increases by (14 ± 4)% for the most central collisions relative to $\sqrt{s_{NN}} = 130$ GeV collisions [6–9], in agreement with the results of the PHOBOS experiment [10]. In highly energetic nuclear collisions, charged particles can be produced by hadronic ("soft") as well as partonic ("hard") collision processes. By extending the $dN_{\rm ch}/d\eta$ systematics to cover a range of reaction centralities and pseudorapidities, it becomes possible to more fully explore the different reaction mechanisms.

The data were obtained using several subsystems of the BRAHMS experiment at RHIC [11]: the Multiplicity Array (MA), the Beam-Beam Counter (BBC) arrays, and the Zero-Degree Calorimeters (ZDCs). An analysis of charged-particle multiplicities for Au + Au reactions at $\sqrt{s_{NN}} = 130$ GeV using a nearly identical procedure to the one presented here is described in Ref. [9].

The MA determines $dN_{\rm ch}/d\eta$ around midrapidity with a modestly segmented Si strip-detector array (SiMA) surrounded by an outer plastic-scintillator tile array (TMA) in a double, hexagonal-sided barrel arrangement. Each of the 25 Si detectors (4 cm × 6 cm × 300 μm) is located 5.3 cm from the beam axis and is subdivided along

the beam direction into seven active strips. The TMA has 35 plastic-scintillator tiles (12 cm × 12 cm × 0.5 cm) located 13.9 cm from the beam axis. The effective coverage of the MA is $-3.0 \leq \eta \leq 3.0$. The SiMA is used alone for determining $dN_{\rm ch}/d\eta$ values near midrapidity because of its higher segmentation. However, both the SiMA and TMA are used for establishing reaction centrality, as discussed below. Particle multiplicities are deduced from the observed energy loss in the SiMA and TMA elements by using GEANT simulations [12] to relate energy loss to the number of particles hitting a given detector element [9]. SiMA and TMA elements are calibrated using low-multiplicity events, where well-defined peaks are observed in the individual energy spectra corresponding to single-particle hits [9].

The BBC arrays consist of two sets of Cherenkov UV-transmitting plastic radiators coupled to photomultiplier tubes. The Cherenkov radiators are positioned around the beam pipe with one set on either side of the nominal interaction point at a distance of 2.20 m. The time resolution of the BBC elements permits the determination of the interaction point with an accuracy of ≈0.9 cm. Charged-particle multiplicities with $2.1 \leq |\eta| \leq 4.7$ are deduced from the number of particles hitting each detector, as found by dividing the measured detector signal by the average response of the detector to a single particle.

The ZDCs are located ±18 m from the nominal interaction point and measure neutrons that are emitted at small angles with respect to the beam direction [13]. Clean selection of minimum-biased events required a coincidence between the two ZDC detectors and a minimum of four "hits" in the TMA. It is estimated that this selection includes 95% of the Au + Au total inelastic cross section.

Reaction centrality is determined by selecting different regions in the total multiplicity distribution of either the MA or the BBC arrays. The distributions are adjusted for "missed" events, as described in Ref. [9]. In determining $dN_{\rm ch}/d\eta$, the centrality dependence of the MA and BBC distributions are based on the total multiplicity measurements of the corresponding array, thus allowing a range of vertex locations to be used in the BBC analysis beyond the acceptance of the MA (see Ref. [9]). For $3.0 \leq |\eta| \leq 4.2$, where it was possible to analyze the BBC data using both centrality selections, the two analyses give results to within 2% of each other. In general, statistical errors on the measurements are less than 1%, with systematic errors of 8% and 10% for the SiMA and BBC arrays, respectively. The systematic errors are dominated by overall scaling uncertainties resulting from the calibration procedures and should primarily lead to a common scale offset for data obtained at the two RHIC energies. However, there may be as much as a 3% relative scale error between the two energies. A point-to-point error is also present, as indicated by the small asymmetry seen in Fig. 1 for the more central collisions.

Figure 1 shows the measured $dN_{\rm ch}/d\eta$ distributions for charged particles for several centrality ranges. The

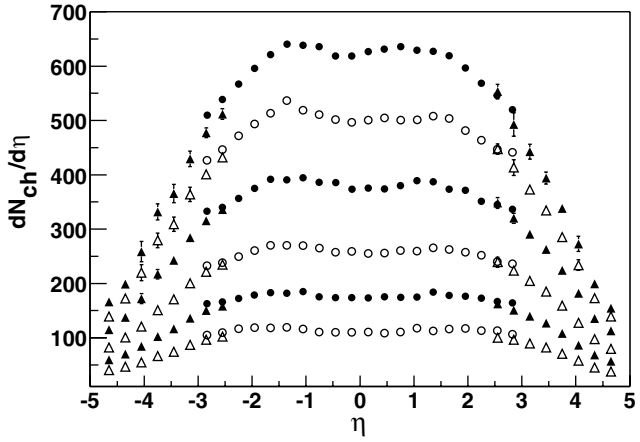

FIG. 1. Distributions of $dN_{\rm ch}/d\eta$ for centrality ranges of, top to bottom, (0−5)%, (5−10)%, (10−20)%, (20−30)%, (30−40)%, and (40−50)%. The SiMA and BBC results are indicated by circles and triangles, respectively. Statistical errors are shown for all points where they are larger than the symbol size.

$dN_{\rm ch}/d\eta$ values for these selected centralities at $\eta = 0$, 3.0, and 4.5 are listed in Table I, together with the average number of participating nucleons $\langle N_{\rm part}\rangle$ estimated from the HIJING (heavy-ion jet interaction generator) model [14] using default parameters. For the most central collisions [(0−5)%], $dN_{\rm ch}/d\eta|_{\eta=0} = 625 \pm 1(\text{stat}) \pm 55(\text{syst})$. This gives a scaled multiplicity value of $(dN_{\rm ch}/d\eta)/\langle N_{\rm part}/2\rangle = 3.5 \pm 0.3$ charged particles per participating nucleon pair and indicates a (13 ± 4)% increase relative to Au + Au reactions at $\sqrt{s_{NN}} = 130$ GeV [9,15]. For the most peripheral collisions analyzed here [(40−50)%], we find $dN_{\rm ch}/d\eta|_{\eta=0} = 110 \pm 10$, resulting in a scaled value of 3.0 ± 0.4. By integrating the (0−5)% multiplicity distribution we deduce that 4630 ± 370 charged particles are emitted in the considered pseudorapidity range. This value is (21 ± 4)% higher than at $\sqrt{s_{NN}} = 130$ GeV [9].

While the scaled multiplicities increase with centrality at midrapidity, Fig. 2 shows they are independent of both collision centrality and beam energy over a pseudorapidity range from 0.5 to 1.5 units below the beam rapidity. This is found for energies ranging from the CERN-SPS energy ($\sqrt{s_{NN}} = 17$ GeV) [16] to the present RHIC beam energy and is consistent with a limiting-fragmentation picture in which the excitations of the fragment baryons saturate at a moderate collision energy, independent of system size [9]. The increased projectile kinetic energy is utilized for particle production below beam rapidity, as evidenced by the observed increase in the scaled multiplicity for central events at midrapidity.

Figure 3 presents the $dN_{\rm ch}/d\eta$ distributions obtained by averaging the values for negative and positive pseudorapidities to further decrease the experimental uncertainties. The solid lines are calculations using the model of Kharzeev and Levin [5]. This model, which is based on a classical QCD calculation using parameters fixed to the $\sqrt{s_{NN}} = 130$ GeV data, is able to reproduce the magnitude

TABLE I. $dN_{\rm ch}/d\eta$ values. Total uncertainties, dominated by the systematics, are indicated. The average number of participants $\langle N_{\rm part}\rangle$ and collisions $\langle N_{\rm coll}\rangle$ is given for each centrality class, with combined model and experimental uncertainties. The model uncertainties are obtained by varying the assumptions for the Glauber picture, including the *NN* cross section and the nuclear radius and surface diffuseness parameters. $N_{\rm ch}$ is the integral charged-particle multiplicity within $-4.7 \le \eta \le 4.7$.

Centrality	$\eta = 0$	$\eta = 3.0$	$\eta = 4.5$	$N_{\rm ch}$	$\langle N_{\rm coll}\rangle$	$\langle N_{\rm part}\rangle$
0–5	625 ± 55	470 ± 44	181 ± 22	4630 ± 370	1000 ± 125	357 ± 8
5–10	501 ± 44	397 ± 37	156 ± 18	3810 ± 300	785 ± 115	306 ± 11
10–20	377 ± 33	309 ± 28	125 ± 14	2920 ± 230	552 ± 100	239 ± 10
20–30	257 ± 23	216 ± 17	90 ± 10	2020 ± 160	335 ± 58	168 ± 9
30–40	174 ± 16	149 ± 14	64 ± 7	1380 ± 110	192 ± 43	114 ± 9
40–50	110 ± 10	95 ± 9	43 ± 5	890 ± 70	103 ± 31	73 ± 8

and shape of the observed multiplicity distributions quite well. The dashed lines are the results of a multiphase transport (AMPT) model [17,18]. This is a cascade model based on HIJING [14], but includes final-state rescattering of produced particles. The AMPT model is also able to account for the general trend of the measured distributions, particularly for the most central collisions. We also plot the similar distributions [19] from $p\bar{p}$ collisions at $\sqrt{s} = 200$ GeV, scaled up by the corresponding number of Au + Au participant pairs, for the (0–5)% and (40–50)% centralities. For central collisions the Au + Au data show a strong enhancement over the entire pseudorapidity range relative to the $p\bar{p}$ results, with an excess of (41 ± 9)% observed at midrapidity. This suggests significant influence of the extended, high-density medium in the case of the heavy-ion collision. The observed enhancement decreases to about 10% for (40–50)% centrality collisions. We also note that the width in pseudorapidity of the measured distributions increases slightly as the centrality decreases, with $\sigma_{\rm rms} = 2.33 \pm 0.02$ and 2.40 ± 0.02 for the (0–5)% and (40–50)% centralities, respectively. This again suggests increased particle production at midrapidity for more central collisions. These values can be compared to $\sigma_{\rm rms} = 2.38 \pm 0.05$ for the $p\bar{p}$ data.

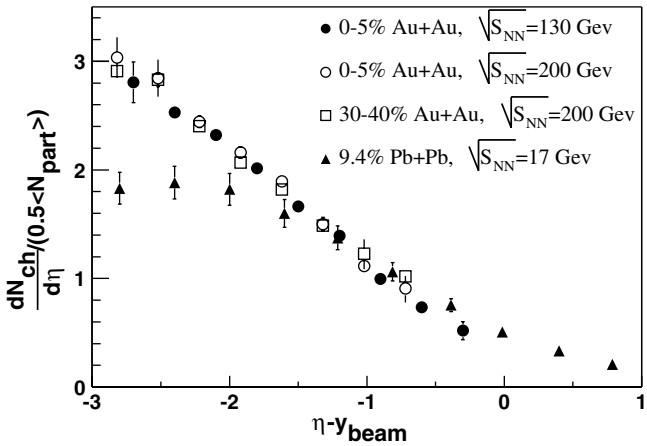

FIG. 2. Charged-particle multiplicities normalized to the number of participant nucleon pairs (see Table I) for the present (0–5)% central (open circles) and (40–50)% central (open squares) Au + Au results at $\sqrt{s_{NN}} = 200$ GeV, the BRAHMS (0–5)% Au + Au results [9] at $\sqrt{s_{NN}} = 130$ GeV (closed circles), and the 9.4% central Pb + Pb data at $\sqrt{s_{NN}} = 17$ GeV (closed triangles) of Ref. [16]. Data are plotted as a function of the pseudorapidity shifted by the relevant beam rapidity. Representative total uncertainties are shown for a few Au + Au points.

The ratios of $dN_{\rm ch}/d\eta$ values measured at $\sqrt{s_{NN}} = 130$ GeV and $\sqrt{s_{NN}} = 200$ GeV for different centralities are shown in Fig. 4. An increase in charged-particle multiplicity as a function of energy for a central-plateau region ($|\eta| < 2.5$) is observed, with a comparable increase of 10% to 20% observed for all centralities. The upturn in the ratios seen at forward rapidities is due to the widening of the multiplicity distribution at the higher energy, consistent with the increase in beam rapidity ($\Delta y = 0.43$). The curves show the corresponding ratios resulting from the two model calculations.

Finally in Fig. 5 we plot $(dN_{\rm ch}/d\eta)/\langle N_{\rm part}/2\rangle$ as a function of the average number of participants $\langle N_{\rm part}\rangle$ for three narrow pseudorapidity regions ($\Delta\eta \approx 0.2$) around $\eta = 0$, 3.0, and 4.5. As already suggested, particle production per participant pair is remarkably constant and near unity at the forward rapidities characteristic of the fragmentation region, while showing a significant increase for the more central collisions with $\eta \approx 0$. The midrapidity behavior has been attributed to the onset of hard-scattering processes which are dependent on the number of binary

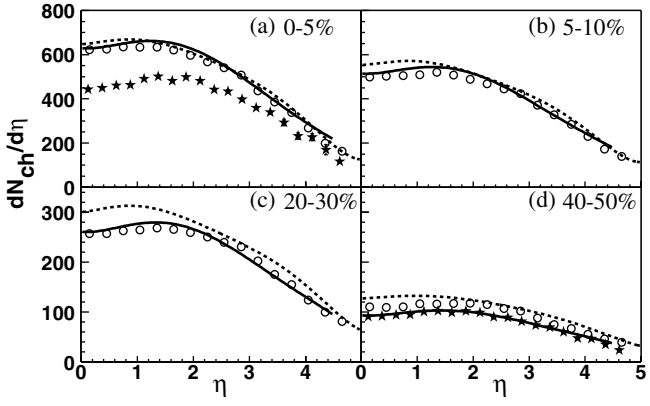

FIG. 3. (a)–(d) Measured $dN_{\rm ch}/d\eta$ distributions for centrality ranges of (0–5)%, (5–10)%, (20–30)%, and (40–50)%. Theoretical predictions by Kharzeev and Levin (solid lines) and by the AMPT model (dashed lines) are also shown. Results from $p\bar{p}$ collisions at $\sqrt{s} = 200$ GeV [19], scaled by the Au + Au values of $\langle N_{\rm part}\rangle/2$, are shown with stars (a),(d).

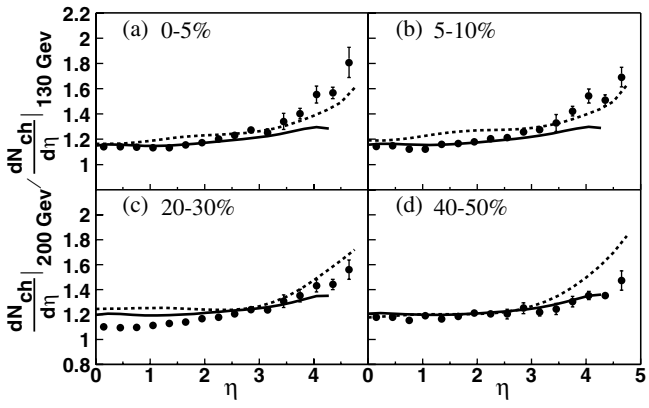

FIG. 4. Ratio of $dN_{\rm ch}/d\eta$ values at $\sqrt{s_{NN}} = 200$ and 130 GeV compared to the model calculations (see Fig. 3 caption). Total uncertainties are shown, assuming a 3% relative scaling uncertainty between the two energies.

nucleon collisions $N_{\rm coll}$ rather than $N_{\rm part}$ [8]. Using $N_{\rm coll}$ and $N_{\rm part}$ values from HIJING [14] we fit the data with a function of the form $dN_{\rm ch}/d\eta = \alpha \cdot N_{\rm part} + \beta \cdot N_{\rm coll}$. For $\eta = 0$ (4.5) we obtain $\alpha = 1.26 \pm 0.09 \pm 0.20$ ($0.66 \pm 0.03 \pm 0.10$) and $\beta = 0.15 \mp 0.04 \mp 0.05$ ($-0.06 \mp 0.01 \mp 0.03$), where the first uncertainty assumes a 3% point-to-point error for the $dN_{\rm ch}/d\eta$ values and the second uncertainty results from the $N_{\rm coll}$ and $N_{\rm part}$ uncertainties. For comparison we find $\alpha = 1.24 \pm 0.08 \pm 0.20$ ($0.55 \pm 0.02 \pm 0.09$) and $\beta = 0.12 \mp 0.04 \mp 0.06$ ($-0.09 \mp 0.01 \mp 0.03$) at $\sqrt{s_{NN}} = 130$ GeV. For central events at $\eta \approx 0$ we find that the hard-scattering component to the charged-particle production remains almost constant, with values of $(20 \pm 7)\%$ and $(25 \pm 7)\%$ at $\sqrt{s_{NN}} = 130$ and 200 GeV, respectively. For this comparison, only the experimental component of the uncertainties is given since the theory uncertainties will be highly correlated at the two energies.

In conclusion, we find that the charged-particle production increases by a constant amount from $\sqrt{s_{NN}} = 130$ GeV to $\sqrt{s_{NN}} = 200$ GeV in a wide region around midrapidity. The data are well reproduced by calculations based on high-density QCD and by the AMPT/HIJING microscopic parton model. A phenomenological analysis in terms of a superposition of soft- and hard-scattering particle production indicates that the hard-scattering component seen at midrapidity for central collisions is not significantly enhanced as compared to the $\sqrt{s_{NN}} = 130$ GeV results. We find good consistency with the gluon saturation model of Kharzeev and Levin, but stress that, within errors of models and data alike, the data can be equally well reproduced by other models that do not require parton-collision saturation. This work establishes a baseline for particle production at the maximum energy currently available for nucleus-nucleus collisions.

We thank the RHIC collider team for their efforts. This work was supported by the Division of Nuclear Physics of the U.S. Department of Energy, the Danish Natural Science Research Council, the Research Council of Norway, the Polish State Committee for Scientific Research (KBN), and the Romanian Ministry of Research. We are grateful to D. Kharzeev, E. Levin, Zi-wei Lin, and H. Heiselberg for useful discussions and model calculations.

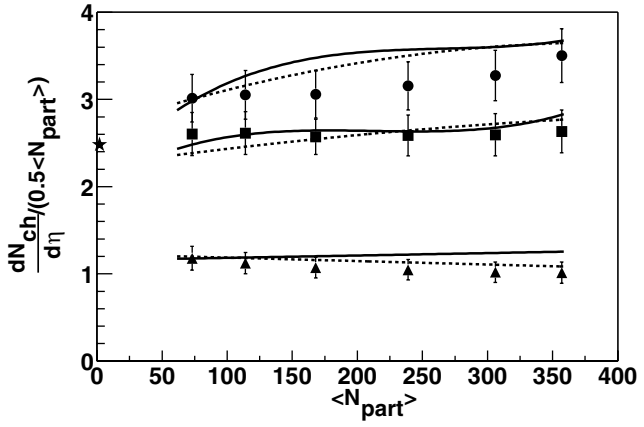

FIG. 5. $dN_{\rm ch}/d\eta$ per participant nucleon pair as a function of the average number of participants (see table) for $\eta = 0$ (circles), 3.0 (squares), and 4.5 (triangles). The curves show the model predictions (see Fig. 3 caption). The star denotes the $p\bar{p}$ result at $\eta = 0$ [19].

*Deceased.

[1] K. Adcox *et al.,* Phys. Rev. Lett. **88**, 022301 (2002).
[2] J. C. Dunlop *et al.,* Nucl. Phys. **A698**, 515c (2002); B. Lasiuk, in Workshop on High p_T Phenomenon at RHIC, BNL, 2002 (unpublished).
[3] L. V. Gribov, E. M. Levin, and M. G. Ryskin, Phys. Rep. **100**, 1 (1983).
[4] K. J. Eskola, K. Kajantie, and K. Tuominen, Phys. Lett. B **497**, 39 (2001).
[5] D. Kharzeev and E. Levin, Phys. Lett. B **523**, 79 (2001); D. Kharzeev (private communication).
[6] B. B. Back *et al.,* Phys. Rev. Lett. **85**, 3100 (2000).
[7] C. Adler *et al.,* Phys. Rev. Lett. **87**, 112303 (2001).
[8] K. Adcox *et al.,* Phys. Rev. Lett. **86**, 3500 (2001).
[9] I. G. Bearden *et al.,* Phys. Lett. B **523**, 227 (2001).
[10] B. B. Back *et al.,* Phys. Rev. Lett. **88**, 022302 (2002).
[11] M. Adamczyk *et al.* (to be published).
[12] GEANT 3.2.1, CERN Program Library.
[13] C. Adler *et al.,* Nucl. Instrum. Methods Phys. Res., Sect. A **470**, 488 (2001).
[14] X. N. Wang and M. Gyulassy, Phys. Rev. D **44**, 3501 (1991).
[15] We have reanalyzed our earlier $\sqrt{s_{NN}} = 130$ GeV data to include only the same set of detectors as used here.
[16] P. Deines-Jones *et al.,* Phys. Rev. C **62**, 014903 (2000).
[17] Bin Zhang, C. M. Ko, Bao-An Li, and Zi-wei Lin, Phys. Rev. C **61**, 067901 (2001).
[18] Zi-wei Lin, Subrata Pal, C. M. Ko, Bao-An Li, and Bin Zhang, Phys. Rev. C **64**, 011902(R) (2001); Zi-wei Lin, Subrata Pal, C. M. Ko, Bao-An Li, and Bin Zhang, Nucl. Phys. **A698**, 375c (2002); Zi-wei Lin (private communication).
[19] G. J. Alner *et al.,* Z. Phys. C **33**, 1 (1986).